Deep-Sea Research II 55 (2008) 1321–1333

Contents lists available at ScienceDirect

Deep-Sea Research II

journal homepage: www.elsevier.com/locate/dsr2

Diatoms in the desert: Plankton community response to a mesoscale eddy in the subtropical North Pacific

Susan L. Brown [a,*], Michael R. Landry [b], Karen E. Selph [a], Eun Jin Yang [c], Yoshimi M. Rii [a], R.R. Bidigare [d]

[a] Department of Oceanography, University of Hawaii at Manoa, 1000 Pope Road, Honolulu, HI 96822, USA
[b] Integrative Oceanography Division, Scripps Institution of Oceanography, University of California at San Diego, La Jolla, CA 92093-0227, USA
[c] Marine Environment Research Department, Korea Ocean Research & Development Institute, Ansan P.O. Box 29, Seoul 425-600, South Korea
[d] Hawaii Institute of Marine Biology, Kaneohe, HI 96744, USA

ARTICLE INFO

Article history:
Accepted 11 February 2008
Available online 15 May 2008

Keywords:
Plankton
Subtropical North Pacific
Eddy
Community structure
Diatoms

ABSTRACT

As part of the E-Flux project, we documented spatial variability and temporal changes in plankton community structure in a cold-core cyclonic eddy in the lee of the Hawaiian Islands. Cyclone *Opal* spanned 200 km in diameter, with sharply uplifted isopycnals (80–100 m relative to surrounding waters) and a strongly expressed deep chlorophyll *a* maximum (DCM) in its central core region of 40 km diameter. Microscopic and flow cytometric analyses of samples from across the eddy revealed dramatic transitions in phytoplankton community structure, reflecting *Opal*'s well-developed physical structure. Upper mixed-layer populations in the eddy resembled those outside the eddy and were dominated by picophytoplankton. In contrast, the DCM was composed of large chain-forming diatoms dominated by *Chaetoceros* and *Rhizosolenia* spp. Diatoms attained unprecedented levels of biomass (nearly 90 $\mu g\, C\, l^{-1}$) in the center of the eddy, accounting for 85% of photosynthetic biomass. Protozoan grazers displayed two- to three-fold higher biomass levels in the eddy center as well. We also found a distinct and persistent layer of senescent diatom cells overlying healthy populations, often separated by less than 10 m, indicating that we were sampling a bloom in a state of decline. Time-series sampling over 8 days showed a successional shift in community structure within the central diatom bloom, from the unexpected large chain-forming species to smaller forms more typical of the subtropical North Pacific. The diatom bloom of Cyclone *Opal* was a unique, and possibly extreme, example of biological response to physical forcing in the North Pacific subtropical gyre, and its detailed study may therefore help to improve our predictive understanding of environmental controls on plankton community structure.

1. Introduction

Size distribution and species composition of plankton assemblages strongly regulate carbon cycling and export from surface waters of the oceans (Michaels and Silver, 1988; Legendre and Le Fevre, 1995; Legendre and Michaud, 1998; Legendre and Rivkin, 2000). Oligotrophic open-ocean ecosystems represent one extreme in the spectrum of natural community variability, with microbial-based food webs that channel the fate of photosynthetic production to respiration, remineralization and dissolved organics. At the other extreme, diatom-based food webs of eutrophic systems are efficient in transferring carbon to higher trophic levels and to carbon export from the photic zone as zooplankton fecal pellets and sinking aggregates. We have sufficient understanding of the underlying controls of plankton community structure to design models that capture the general flavor of these ecosystem types (Boyd and Doney, 2002; Le Quéré et al., 2005), and to manipulate natural systems in directions intended to enhance carbon export and sequestration (Coale et al., 1996, 2004; Boyd and Law, 2001; Tsuda et al., 2003; Harrison, 2006). However, our understanding of the range of variability within ecosystems, the small-scale phenomena and processes that drive variability, and their implications for carbon cycling and export is rudimentary at best.

Phytoplankton standing stock is characteristically low in the North Pacific subtropical gyre (NPSG), with photosynthetic bacteria and nanoflagellates typically dominating the autotrophic community (Karl et al., 2001) and with species composition exhibiting "unusual stability relative to other ecosystems" (Venrick, 1999). The relatively stable assemblage of small cells in this archetypical oligotrophic region, once characterized as a "biological desert", provides an ideal backdrop for assessing community perturbation responses to mesoscale physical phenomena, like eddies and Rossby waves, that periodically infuse the

* Corresponding author. Fax: +1 808 956 7709.
E-mail address: sbrown@soest.hawaii.edu (S.L. Brown).

0967-0645/$ - see front matter © 2008 Elsevier Ltd. All rights reserved.
doi:10.1016/j.dsr2.2008.02.012

euphotic zone with nutrients (Brzezinski et al., 1998; Cipollini et al., 2001; Uz et al., 2001; Sakamoto et al., 2004).

The E-Flux study was designed to test the hypothesis that nutrient infusions from cyclonic eddies in the lee of the Hawaiian Islands alter plankton community structure, increase productivity, and ultimately enhance carbon export in the NPSG (Benitez-Nelson et al., 2007). Hawaiian lee cyclones form regularly where gaps in island topography focus trade winds (Patzert, 1969; Lumpkin, 1998; Chavanne et al., 2002). They are therefore predictable and persistent features for investigating the ecological and biogeochemical responses to eddy forcing. The wind-driven eddy field in the lee of the Hawaiian Islands is likely to be modified by climate change with consequences for recruitment process and local fisheries (Lobel and Robinson, 1986; Seki et al., 2002). A clear understanding of the effects of mesoscale eddies on plankton community structure is therefore of regional interest and importance.

The objectives of this study were to investigate spatial variability and temporal changes in plankton community composition and size structure in a first baroclinic, cold-core eddy that developed in the lee of Hawaii and Maui in February 2005 (Benitez-Nelson et al., 2007). Cyclone *Opal*, named for its dramatic subsurface bloom of large diatoms, was an especially well-developed and mature eddy of ~4–5 weeks in age, based on satellite imagery (Nencioli et al., 2008) when it was studied on the third E-Flux cruise (E-Flux III) from 10 to 28 March. It spanned over ~200 km in diameter with an intense doming of isopycnals and a core of lower temperature water that reached the surface (Nencioli et al., 2008). Cyclone *Opal* represented a major nutrient perturbation to this subtropical oligotrophic region, and therefore an important opportunity to investigate spatial and temporal relationships in the plankton community response.

2. Materials and methods

2.1. Sampling

To assess spatial variability of plankton community structure and biomass in Cyclone *Opal*, seawater samples were collected at eight depths from 11 stations along a 200 km NE–SW transect through the eddy (Fig. 1; 13–14 March 2005). Following transect sampling, we documented the temporal evolution of the community over an additional 6 days (16–21 March) as the eddy migrated SW at a mean translational speed of ~8 km d^{-1} (Dickey et al., 2008). Approximate daily sampling during this period (seven depths from 10 to 125 m, down to ~0.5% light level) was confined to the central core region *of Opal* (IN stations), as determined by real-time ADCP velocities and *in situ* temperature anomalies (Nencioli et al., 2008). For comparative purposes, similar sampling was subsequently completed at three control stations outside of the eddy influence (OUT stations, 24–26 March; Fig. 1). At all stations, a similar suite of samples was collected for community analyses by flow cytometry, pigments and microscopy.

2.2. Picoplankton analyses by flow cytometry

Duplicate samples (1 ml) for flow cytometric analysis of heterotrophic and photosynthetic bacteria (*Prochlorococcus* and *Synechococcus*) were preserved with paraformaldehyde (0.5% final concentration) and flash frozen in liquid nitrogen. On shore, samples were stored in a −85 °C freezer until analysis. Replicate samples were thawed and stained with Hoechst 34442 (1 μg/ml, final concentration) for 1 h at room temperature in the dark

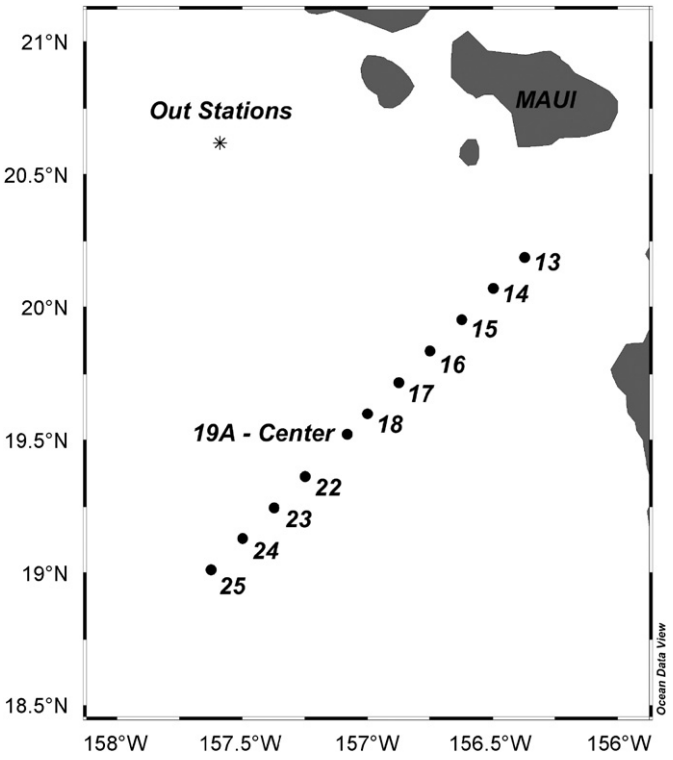

Fig. 1. Map of the E-Flux III study area in the lee of the Hawaiian Islands showing the spatial extent of Transect 3 through Cyclone *Opal*. Transect station numbers are indicated and 19A marks the center of the eddy.

(Monger and Landry, 1993; Campbell and Vaulot, 1993; Campbell et al., 1994). Internal standards of auto-fluorescent polystyrene beads were added to each sample to normalize scatter and fluorescence signals. Populations were analyzed with a Beckman-Coulter Altra flow cytometer equipped with two argon ion lasers, one tuned to deliver 1 W of 488 nm light and the other 200 mW of UV excitation. Sample flow rate (50 μl/min) was controlled with a Harvard Apparatus syringe pump. Scatter (side and forward), and fluorescence signals were collected using filters for Hoechst-bound DNA, phycoerythrin and chlorophyll. Data was generated as listmode files (FCS 2.0 format) with Expo32 software (Beckman-Coulter). Population designations, based on the scatter and fluorescence signals, were derived from listmode files using FlowJo software (Tree Star Inc., www.flowjo.com). Flow cytometrically determined populations were converted to "biomass" equivalents assuming cellular carbon values of 11, 32–60 (depending upon relative scattering properties), and 101 fg C $cell^{-1}$ for heterotrophic bacteria (HBACT), *Prochlorococcus* spp. (PRO) and *Synechococcus* spp. (SYN), respectively (Garrison et al., 2000).

2.3. Microscopical analyses of nano- and microplankton

Aliquots of 50 and 250–500 ml were collected for analyses of nano- and micro-plankton by digitally enhanced epifluorescence microscopy. Sub-samples of 50 ml were preserved with paraformaldehyde (0.5% final concentration) and stained with proflavin (0.33%, w/v). Sub-samples of 250 ml were preserved with 250 μl of alkaline Lugol's solution followed by 5 ml of formalin and 125 μl of sodium thiosulfate (modified protocol from Sherr and Sherr, 1993); and then stained with proflavin (0.33%, w/v). Preserved samples were allowed to fix at room temperature for at least 1 h prior to filtration. Samples were then slowly (~5 psi) filtered onto black 0.8 μm (50 ml) or 8.0 μm (250 ml) Nuclepore filters overlaying 20 μm Millipore backing

filters to facilitate even cell distributions. During filtration, the samples were drawn down until ~5 ml remained in the filtration tower. Concentrated DAPI (50 mg ml^{-1}) was then added and allowed to sit for 5 s before filtering the remaining sample until dry. Filters were mounted onto glass slides with immersion oil and cover slips. Slides were viewed and digitized on shipboard with an inverted Olympus IX71 microscope configured with an epifluorescence kit, a 100 W power supply, an F mount, and MacroFire color camera. Slides were viewed at either 400× (50-ml aliquots) or 200× (250-ml aliquots), and at least 60 random fields per slide were captured and downloaded to a computer by Picture Frame software. Counting and sizing of cells >1.2 μm length was automated with ImagePro software. Cells were identified and grouped manually. Autotrophic cells were distinguished from heterotrophs by the presence of chlorophyll, seen as red fluorescence under blue light illumination. Length and width measurements were converted to biovolumes (BV; μm^3) by applying appropriate geometric shapes. Carbon biomass was computed from biovolumes based on modified Strathmann (1967) equations for diatoms ($\log_{10} C = 0.76(\log_{10} BV) \times 0.352$) and non-diatom phytoplankton ($\log_{10} C = 0.94(\log_{10} BV) \times 0.60$) (Eppley et al., 1970). Empty diatom frustules (lacking chlorophyll and cytoplasm) were not included in biomass estimates.

Additional samples were collected for analyzing larger and more delicate components of the microplankton community (e.g., ciliated protozoa). Aliquots of 250 ml were preserved with acid Lugol's solution (final concentration 1%) and stored at room temperature in the dark. Sub-samples ranging from 40 to 200 ml, depending on the density of cells, were added to Uttermöhl sedimentation chambers and allowed to settle for at least 48 h. Samples were then counted and measured with a Zeiss inverted microscope. To estimate carbon biomass of protists, cell volumes were calculated by measuring cell dimensions with an ocular micrometer (Edler, 1979). Biomass calculations for Sarcodina were determined from the equation of Michaels et al. (1995). The following conversion factors and equations were used to convert cell volumes into carbon based biomass estimates: 0.19 μg C μm^{-3} for naked ciliates (Putt and Stoecker, 1989); carbon (pg) = 44.5+0.053 lorica volume (μm^3) for loricate ciliates (Verity and Langdon, 1984); carbon (pg) = 0.216 × [volume, μm^3]$^{0.939}$ for heterotrophic dinoflagellates (Menden-Deuer and Lessard, 2000) and carbon (pg) = 0.288 × [volume, μm^3]$^{0.811}$ for diatoms (Menden-Deuer and Lessard, 2000).

2.4. Pigment analyses

Chlorophyll *a* was analyzed using a Varian 9012 HPLC system and methods described in Bidigare et al. (2005). Filters were extracted in 3 ml of HPLC-grade acetone in culture tubes along with 50 μl of an internal standard (canthaxanthin) at 4 °C for 24 h. Photosynthetic pigments were separated on a reverse-phase Waters Spherisorb® 5-μm ODS-2 (4.6 × 250 mm^2) C_{18} column with a corresponding guard cartridge (7.5 × 4.6 mm^2) and a Timberline column heater (26 °C) (Wright et al., 1991; Bidigare et al., 2005). Separated pigments were detected and data were transferred via SpectraSYSTEM Thermo Separation Products UV2000 (dual wavelength UV–vis) and FL2000 (fluorescence) detectors. Chlorophyll identifications were based on absorbance spectra, co-chromatography with standards, and relative retention time. Peak identity was determined by comparing retention times with a chlorophyll *a* standard and representative culture extracts. Spectra-Physics WOW® software was used to conservatively calculate peak area (Mantoura and Llewellyn, 1983; Wright et al., 1991; Bidigare and Trees, 2000).

2.5. Contour plots

Contour plots were generated using Ocean Data View (Schlitzer, 2006). A VG gridding algorithm was used for variable resolution in a rectangular grid where grid spacing varies accordingly to data density.

3. Results

3.1. Depth distribution of phytoplankton biomass across Cyclone Opal

In transect sampling across Cyclone *Opal*, the depth distribution of chlorophyll *a* (Chl *a* = the sum of monovinyl and divinyl Chl *a*) largely reflected the doming of isopycnals (Fig. 2). The Chl *a* maximum (chl max) resided at about 125 m at the eddy edges and OUT stations, with elevated concentrations broadly spanning the sigma-t isopycnal density surfaces from 23.4 to 24 kg m^{-3}. The maximum was uplifted to about 60 m in the eddy center (Stn 19A), where it was narrowly bounded by sigma-t surfaces of 24.2–24.4 kg m^{-3}. Chl *a* concentration in the central subsurface maximum exceeded 1 μg chl l^{-1}, four-fold higher than the transect edges (Stns 13 and 25) and two-fold higher than OUT stations. In contrast, Chl *a* concentration was low and fairly uniform across the eddy in the upper 40 m (Fig. 2, Table 1).

Carbon based estimates of phytoplankton biomass were notably elevated in the center of Cyclone *Opal*, with a maximum concentration of 101 μg C l^{-1} at the chl max (Fig. 2) compared to a mean maximum biomass of 12 μg C l^{-1} at OUT stations (Table 1) and even lower concentrations at the transect edges (chl max ~6.7 μg C l^{-1}). The area of strong eddy-enhanced photosynthetic biomass was confined to a central core region of ~40 km diameter (Nencioli et al., 2008), and primarily restricted to the subsurface chl max. However, carbon biomass was also enriched 1.5-fold in near-surface waters of the central region relative to the transect edges and OUT stations.

The higher phytoplankton biomass in Cyclone *Opal* was composed mainly of diatoms, which represented 85% of the living biomass in the core region and a maximum of 89 μg C l^{-1} at the chl max, compared with <1 μg C l^{-1} at OUT stations (Table 1). Although the diatom bloom was largely confined to the chl max, a smaller, but notable enhancement of 3 μg C l^{-1} was also evident in surface waters across the transect. Two large centric genera, *Rhizosolenia* spp. and *Chaetoceros* spp. dominated the eddy bloom, accounting for 35–45% of diatom biomass. The remaining assemblage consisted of a variety of pennate and chain-forming centric species, nearly all of which exceeded 20 μm in length. The enriched diatom populations in surface waters comprised a different suite of species, primarily *Mastogloia* spp. and *Richelia*–*Rhizosolenia* complexes, more typical of ambient oligotrophic waters.

The eddy core region was also unusual in the presence of a distinct layer of seemingly senescent diatoms overlying healthy populations. In the eddy center at Stn 19A, for example, the biovolume of diatom frustules at 50 and 60 m was equivalent to biomass estimates of 79 and 89 μg C l^{-1}, respectively. However, 85% of the frustules lacked chlorophyll and proflavin-stained protein, leaving only ~12 μg C l^{-1} of carbon biomass as healthy cells at 50 m. The layer of empty ghost cells was a persistent feature in the center of the eddy throughout the study.

For autotrophic eukaryotes other than diatoms (AEUK), biomass was relatively similar across Cyclone *Opal* in the upper 40 m, averaging 6.7 μg C l^{-1} compared to 8 μg C l^{-1} in the center (Stn 19A; Fig. 2, Table 1). In the chl max, AEUK biomass was ~2× higher at Stn 19A compared to transect and OUT stations (Table 1). In contrast to diatoms, subsurface maxima in AEUK biomass were

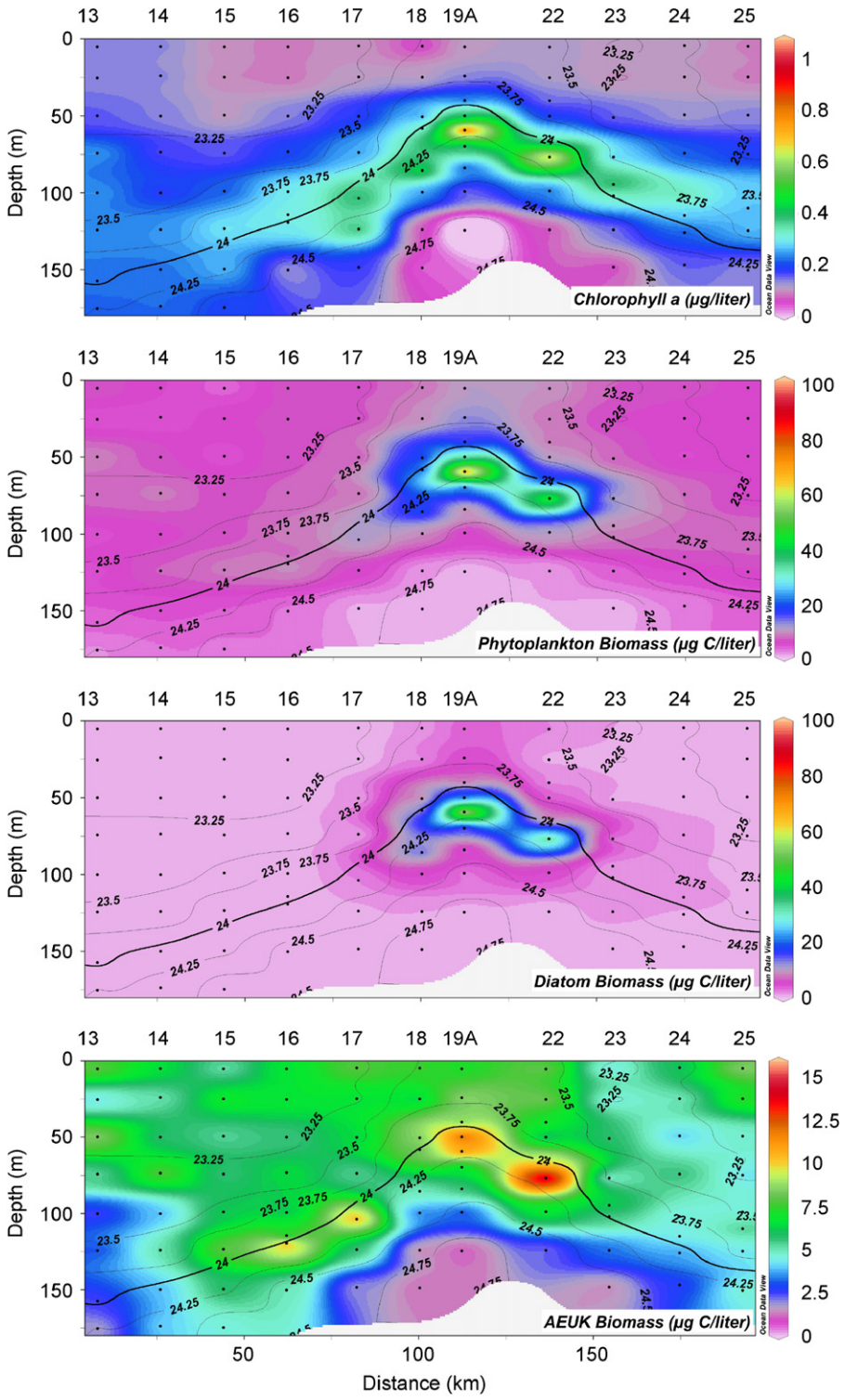

Fig. 2. Distribution of phytoplankton biomass across the eddy. Top panel is chlorophyll *a* ($\mu g\,l^{-1}$) derived from HPLC analyses. Next three panels represent total phytoplankton biomass, diatom biomass and the biomass of autotrophic eukaryotes other than diatoms, respectively, all in $\mu g\,C\,l^{-1}$. Biomass is estimated from microscopy.

frequently observed well away from the eddy center between the sigma-t density surfaces of 24–24.2 $kg\,m^{-3}$.

3.2. Eddy effects on prokaryotic populations

While biomass of eukaryotic phytoplankton, especially diatoms, was strongly enhanced in the lower euphotic zone at the center of Cyclone *Opal*, the eddy effect on photosynthetic prokaryotes, *Prochlorococcus* (PRO) and *Synechococcus* (SYN), was principally evident as uplifted distributions (Fig. 3). Cell abundances of PRO and SYN at the depth of the chl max were lower in the eddy center compared to the transect mean and OUT stations (Table 1b). Population abundances in the upper 40 m were slightly higher for PRO at the central station than the eddy average, though not for SYN (Table 1a). However, both populations were

Table 1

	Average	Station 19A	OUT
(a) Standing stocks of microbial community components and Chl *a* in the upper 40 m across Transect 3 of Cyclone *Opal*			
HBACT (cells ml^{-1})	7.4×105	8.2×105	6.8×105
PRO (cells ml^{-1})	7.0×104	9.8×104	1.3×105
SYN (cells ml^{-1})	2.1×103	2.0×103	2.1×103
Chl *a* ($\mu g\,l^{-1}$)	0.11	0.14	0.08
Diatoms ($\mu g\,C\,l^{-1}$)	3.5	4.2	0.2
AEUK ($\mu g\,C\,l^{-1}$)	6.7	8	3.9
Phyto biomass ($\mu g\,C\,l^{-1}$)	9.4	13.1	8.4
Grazer biomass ($\mu g\,C\,l^{-1}$)	8.1	12.4	4.6
(b) Standing stocks at the depth of the chlorophyll maximum			
HBACT (cells ml^{-1})	4.4×105	6.9×105	4.6×105
PRO (cells ml^{-1})	8.2×104	7.4×104	1.4×105
SYN (cells ml^{-1})	450	<100	664
Chl *a* ($\mu g\,l^{-1}$)	0.35	1.08	0.46
Diatoms ($\mu g\,C\,l^{-1}$)	6.6	89.3	0.7
AEUK ($\mu g\,C\,l^{-1}$)	6.2	12.1	6.3
Phyto biomass ($\mu g\,C\,l^{-1}$)	14.1	101.7	12.3
Grazer biomass ($\mu g\,C\,l^{-1}$)	6.8	15.0	5.9

OUT refers to three stations outside the influence of the eddy. Abundance and biomass were averaged over 40 m to represent surface waters; this layer did not include chlorophyll or biomass maxima.

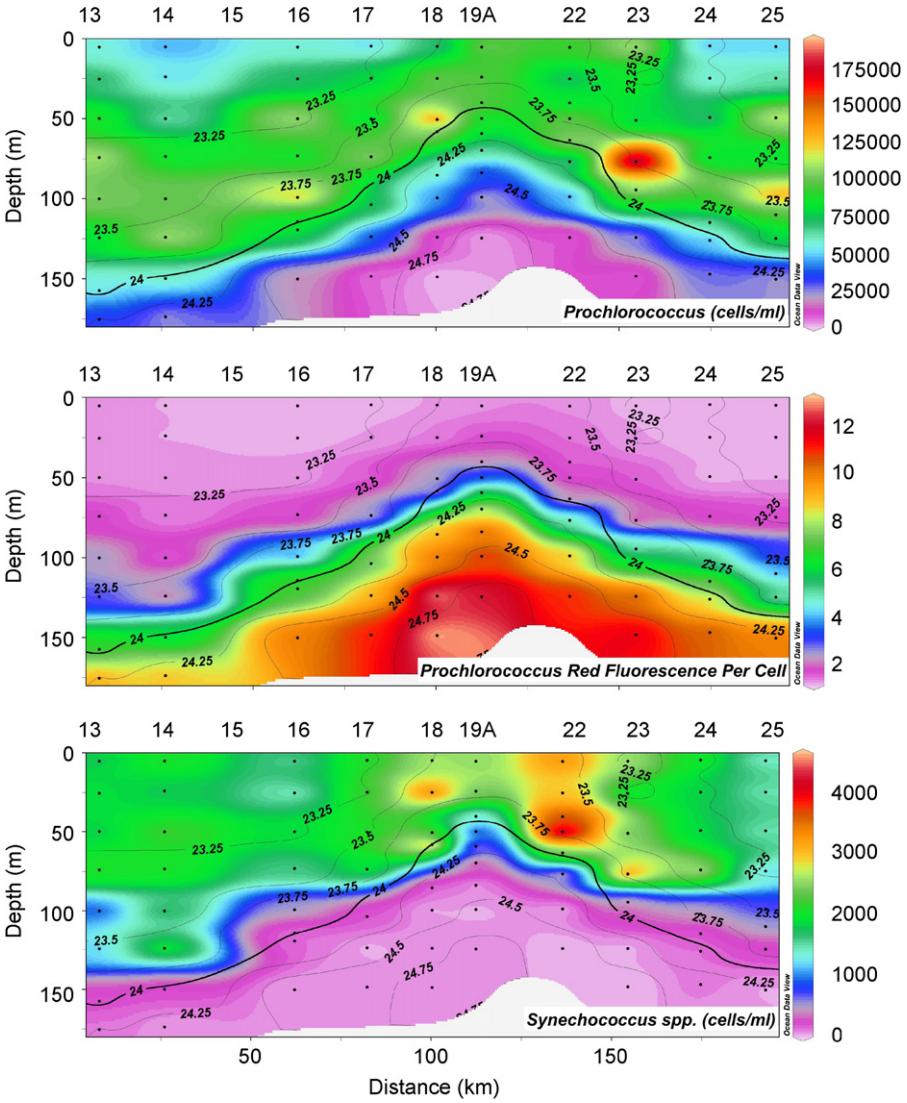

Fig. 3. Contour plots of photosynthetic bacterial abundances. Top panel is numerical abundance of *Prochlorococcus* spp. in cells ml^{-1}; the middle panel represents corresponding red fluorescence per cell, both estimated from flow cytometry. Bottom panel represents the spatial distribution of *Synechococcus* spp. (cells ml^{-1}).

less abundant in the upper euphotic zone of Cyclone *Opal* than at OUT stations, and their population maxima occurred at stations adjacent to rather than at the eddy center (Fig. 3). In addition to cell abundance, red fluorescence of PRO, a proxy for cellular Chl *a* content, reflected the shoaling of isopcynals in Cyclone *Opal* (Fig. 3). The brighter PRO cells in the eddy center are at least partially explained by the uplifting of deep-living populations with larger size and pigment content, but physiological adjustment in response to greater nutrient availability may also have contributed to increased Chl *a* content of cells in the upper mixed layer.

Abundances of non-pigmented prokaryotes (HBACT) were fairly uniform in the upper 40 m (Fig. 4, top panel), averaging 7.4×10^5 cells ml^{-1} (Table 1a). Highest densities of HBACT were found at 40–50 m in the eddy center (Stn 19A), above the depth of the chl max but overlapping the stratum of senescent diatoms (Fig. 4). Relative to OUT stations, HBACT abundances in the upper 40 m were somewhat enhanced in Cyclone *Opal*, but higher, on average, outside the eddy in the chl max (Table 1b). The central eddy region, from Stns 18–22 stands out in terms of HBACT cellular DNA content (measured as blue fluorescence of Hoechst stained cells), suggestive of increased activity and growth rate, especially at and below the core chl max. Forward angle light scatter (FALS), a proxy for cell size (Binder and DuRand, 2002a, b; DuRand and Olson, 1996, 1998), was locally highest in the depth stratum of high diatom biomass (40–60 m) and lowest in central waters immediately below (80–100 m; Fig. 4).

3.3. Temporal evolution of the Cyclone Opal bloom

Using the initial transect sampling as the time zero ($t = 0$) estimate of community standing stock, phytoplankton biomass declined by 80% in the center of Cyclone *Opal* as we tracked and repeatedly sampled the eddy over the course of 8 days (Fig. 5). Relative to initial values, most of the observed decline occurred for diatoms in the chl max depth range, following a slow downward shift of the depth distribution of diatom biomass (Fig. 5). In addition, a species transition was apparent in the diatom assemblage, with *Hemiaulaus* and *Mastogloia* spp. more typical of the region, appearing and replacing the larger bloom dominants, and *Mastogloia* often colonizing senescent *Chaetoceros* frustules. At the time of our last sampling, however, diatom biomass in the chl max ($\sim 12\ \mu g\ C\ l^{-1}$) was still 10-fold higher than ambient concentrations.

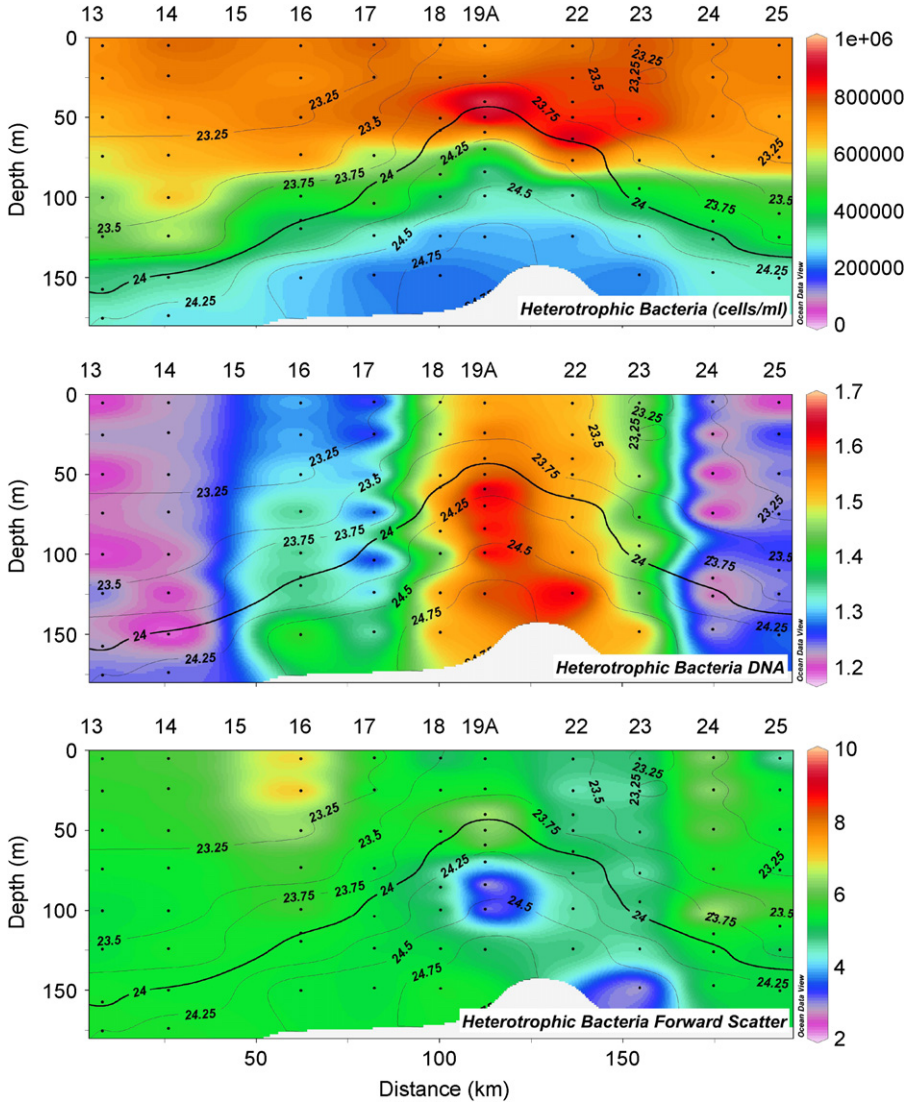

Fig. 4. Spatial distribution of heterotrophic bacteria cell properties as determined by flow cytometry. Top panel shows numerical abundance in cells ml^{-1}. Middle panel represents Hoescht-stained DNA fluorescence, and bottom panel shows normalized forward angle light scattering (FALS), a proxy for cell size; both are in relative units.

During the general decline in large diatoms, autotrophic eukaryotes $<5\,\mu m$ in size remained relatively constant for the euphotic zone as a whole, declining somewhat in the upper 40 m while increasing at depth (data not shown). Total biomass of AEUKs declined by more than half during the time-series sampling and was similar to ambient (OUT) concentrations, with no obvious peak in the upper 100 m, by day 8 (Fig. 5). Through not dominant in AEUK biomass, the prymnesiophyte *Phaeocystis* spp., in both colonial and solitary form, was a consistent component of the chl max community throughout the bloom decline.

In contrast to eukaryotic groups, photosynthetic bacteria generally increased in the eddy center during the bloom decline, although abundances were lower on the last sampling day (Fig. 6). Despite these increases, however, neither PRO nor SYN achieved the total depth-integrated population abundances or deep abundance maxima characteristic of OUT stations. HBACT abundances were relatively constant in surface waters over the time-series sampling, and between IN and OUT stations. Relative to the OUT station mean, HBACT abundances in the eddy exhibited a prominent subsurface peak varying from 50 to 90 m and generally following the depth distribution of phytoplankton (diatom) biomass (Fig. 6).

3.4. Protistan grazers

In Cyclone *Opal* transect sampling, the distribution of protozoan grazers generally followed phytoplankton biomass, reflecting a predator–prey response rather than uplifted grazer populations from below (Fig. 7). Biomass was enhanced by $\sim 3\times$ in the eddy core region in the both the upper 40 m and the chl max (Table 1). Biomass of small heterotrophic flagellates ($<5\,\mu m$), presumably grazers of prokaryotic populations, were higher throughout the water column in the eddy center, whereas larger ciliated protozoa were more strongly associated with the surface and chl max (Fig. 7), including areas of higher AEUK biomass away from the eddy center.

During time-series sampling, protistan grazers initially showed biomass increases at both the surface and the chl max (Fig. 8). The surface population declined by day 4, while biomass peaks remained at depth. Small grazers ($<5\,\mu m$) were more variable with depth, presumably in response to (or the cause of) variability in prokaryotes, namely PRO and HBACT. Ciliate biomass decreased rapidly after the initial sampling, with total grazer biomass and component populations declining by $\sim$50% overall.

4. Discussion

The present data are unique in that we were able to sample, spatially and temporally, the evolving response of a microbial community to a significant nutrient perturbation event within the context of concurrent physical and biogeochemical observations. The analysis is complicated, however, by the complex physical

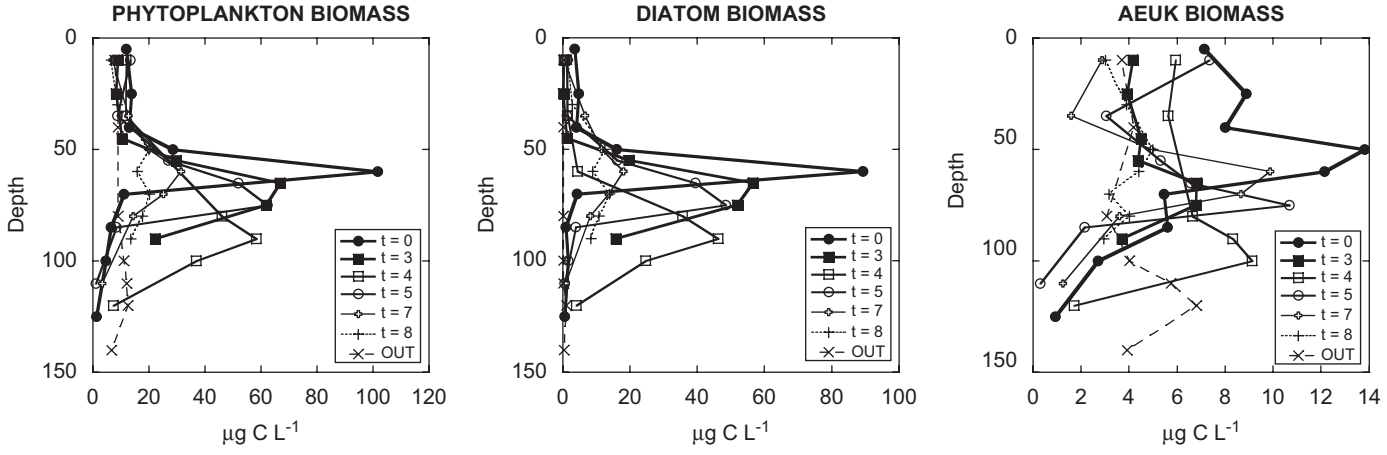

Fig. 5. Temporal evolution of phytoplankton biomass ($\mu g\,C\,l^{-1}$) over a 9-day period. Note different scale on *x*-axis.

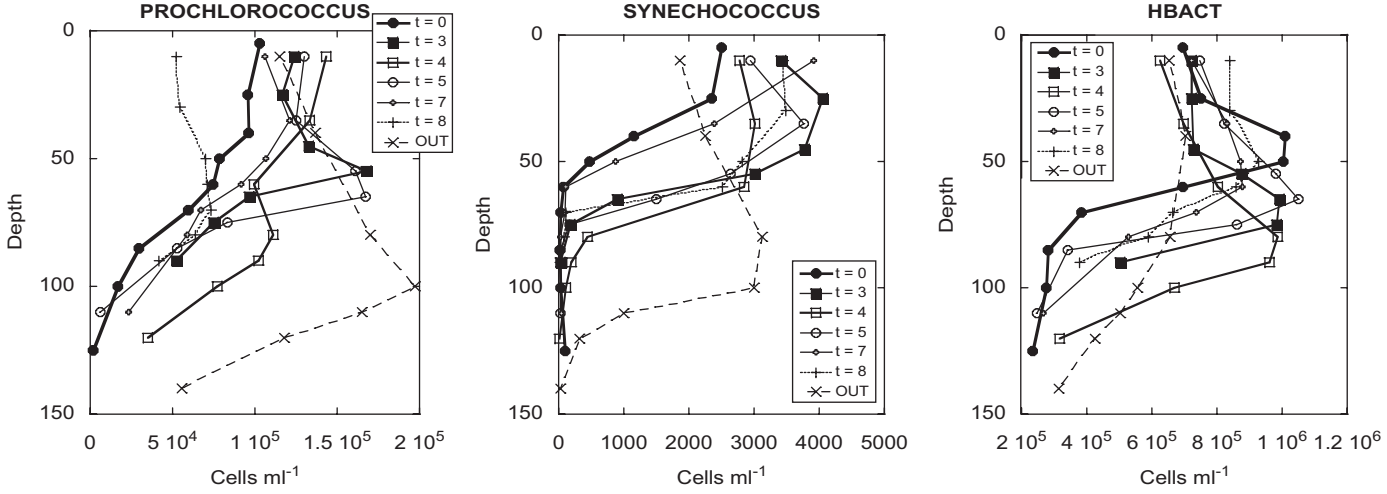

Fig. 6. Temporal evolution of bacterial abundances ($cells\,l^{-1}$). Note different scale on *x*-axis.

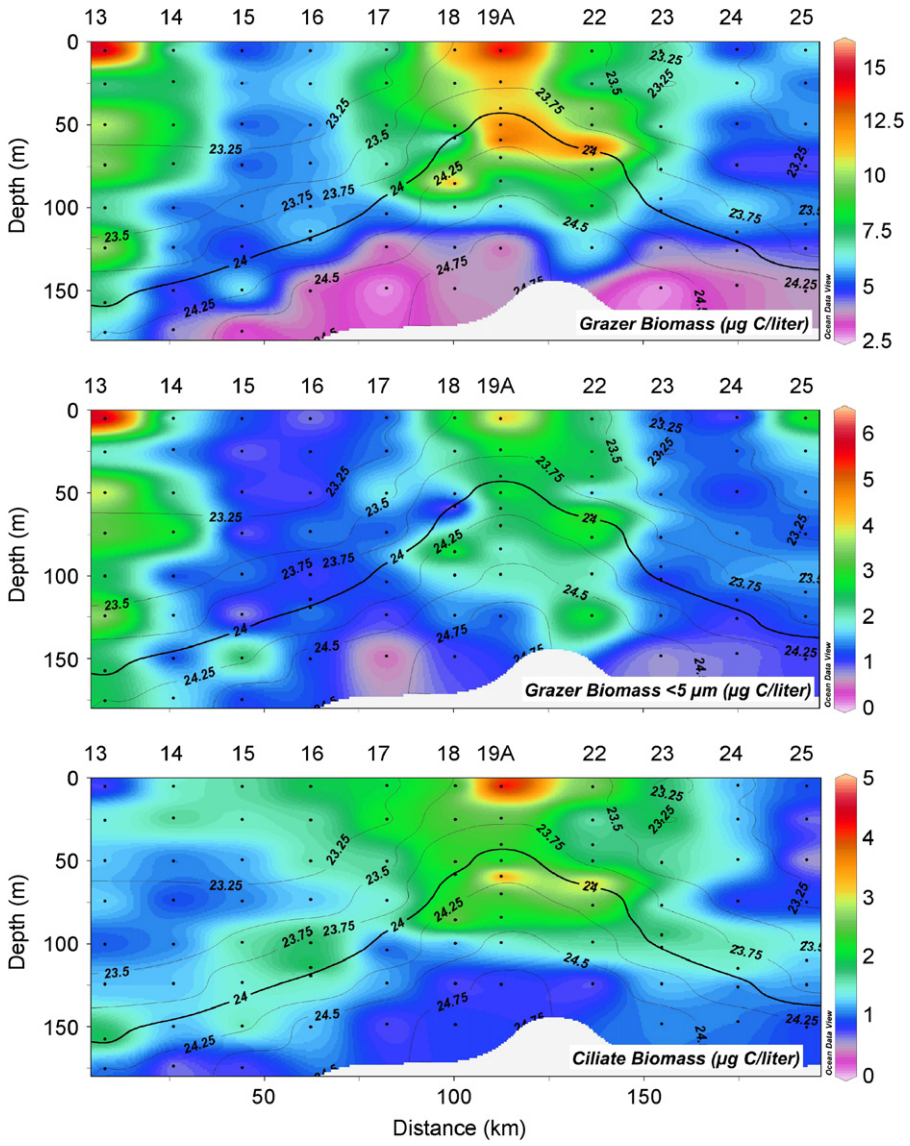

Fig. 7. Spatial distribution of grazer biomass. The top panel shows total grazer abundance in $\mu g\,C\,l^{-1}$. The middle contour represents the biomass of grazers $<5\,\mu m$ in length and the bottom panel is the total biomass of ciliated protozoa, both in $\mu g\,C\,l^{-1}$.

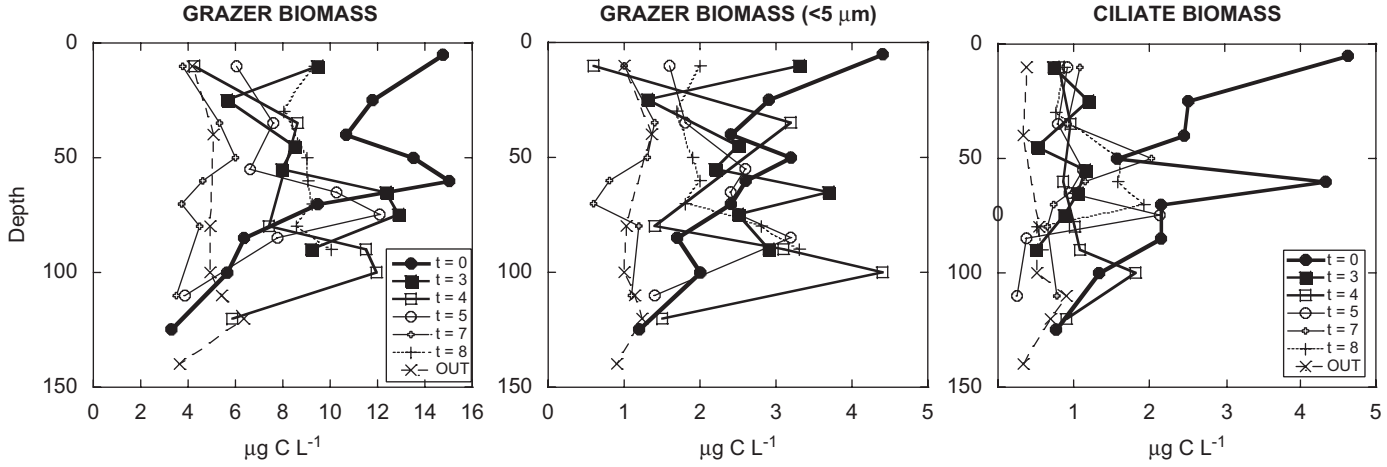

Fig. 8. Temporal evolution of grazer biomass ($\mu g\,C\,l^{-1}$). Note different scale on *y*-axis.

structure of the eddy and the variability in populations with depth. The migration of the eddy further confounds interpretation, as the nominal center of the eddy was a moving target with little surface manifestation (Nencioli et al., 2008). Despite such challenges, several patterns emerge with respect to the plankton response.

4.1. Physical forcing

In Cyclone *Opal*, sigma-$t = 24\,kg\,m^{-3}$ defined the base of the upper mixed layer in the central region, where it was uplifted 80–100 m relative to surrounding waters (Nencioli et al., 2008). The doming isopycnals therefore brought deep water containing light-limited phytoplankton and abundant preformed nutrients into the well-lit euphotic zone, creating an environment conducive to rapid growth and biomass accumulation. The observed vertical layering of diatoms in Cyclone *Opal* is consistent with this mechanism. The uppermost layer of the chl max would have been the first to experience the higher light and the first to bloom and exhaust nutrients, creating the observed upper layer of senescent cells and reducing light penetration to waters below. As this upper layer of the bloom declined and the waters cleared, more light was available for downward growth of the bloom into the underlying nutrient-rich waters.

Besides stimulating the subsurface diatom bloom, nutrients from the uplifted nutricline also affected phytoplankton dynamics in the upper mixed layer of Cyclone *Opal* (Rii et al., 2008). Although not as dramatic as at depth, phytoplankton biomass was $3\times$ higher in the eddy center than in ambient waters, and the response was principally due to diatoms (Table 1). Additionally, mixed-layer populations in the eddy center had higher F_v/F_m, indicative of enhanced photosynthetic efficiency (Bibby et al., 2008), and growth rates (Landry et al., 2008) relative to OUT stations. Mixed-layer abundances of PRO and SYN were similar or lower in the center of *Opal* compared to OUT stations; however, fluorescence per cell and growth rates of PRO were elevated in the eddy relative to OUT conditions (Landry et al., 2008).

Nencioli et al. (2008) reported that a small, shallow portion of Cyclone *Opal* (50 km wide by 70 m deep) was characterized by constant angular velocity, essentially rotating as a solid body isolated from fluid exchange with the surrounding water. The localized response of the diatom bloom is consistent with an isolated parcel of water and appears to be contained within this cylindrical core. The chl max in this region was confined to a narrow depth stratum between sigma-t isopycnal surfaces of 24.2 and $24.4\,kg\,m^{-3}$ (Rii et al., 2008). Nencioli et al. (2008) further hypothesized radial exchange of water along isopycnal surfaces below and outside of this core region, which is consistent with the occurrence of the more diffuse chl max layer spanning a broader range of isopycnals (sigma-t = $23.0–24.4\,kg\,m^{-3}$), as well as enhanced phytoplankton biomass at 100–130 m surrounding the eddy center. PRO appeared to follow a similar pattern with enhanced abundance along isopycnal surfaces beyond the center region.

In general, heterotrophic populations in the eddy developed in response to increases in phytoplankton prey rather than a simple uplifting of ambient populations to shallower depths. High grazer biomass was constrained to the eddy center in accordance with the concept of an isolated core of water. High ciliate biomass extended to deeper depths on either side of the center presumably in response to the greater availability of AEUK prey. The eddy response of HBACT did not follow isopycnal surfaces, but higher abundances were localized in the higher biomass center of the eddy.

The decline of the diatom bloom likely resulted from depletion of silicic acid, an essential nutrient for diatom growth. Silica concentrations in the eddy core were below the limit of detection ($<0.35\,\mu M$) in the chl max, and Si:N ratios were <1, indicative of Si limitation (Rii et al., 2008). Assuming that the core functioned as a solid rotating body, the diatom populations in the upper portion of the subsurface Chl *a* max would have been isolated from additional nutrient inputs.

The migration of the biomass maximum deeper in the water column as the bloom declined (Fig. 5) suggests a relaxation of doming isopycnals. However, sigma-t = $24\,kg\,m^{-3}$ remained at ~55 m, consistent with other signs that the physical structure of the eddy did not change appreciably during the study (Dickey et al., 2008). The deepening biomass distribution is therefore attributable to cells sinking after nutrient exhaustion or to downward growth of the bloom as allowed by light (Benitez-Nelson et al., 2007).

4.2. An anomalous eddy?

Compared to other Hawaiian lee cyclones, the physical structure of *Opal* was quite typical (Nencioli et al., 2008). Biologically, however, *Opal*'s phytoplankton community showed little similarity to five cyclonic lee eddies studied previously: 1989 eddy, *Mikalele*, *Loretta*, *Haulani* and *Noah* (Falkowski et al., 1991; Olaizola et al., 1993; Allen et al., 1996; Seki et al., 2001; Bidigare et al., 2003; Vaillancourt et al., 2003; Rii et al., 2008). While not a large dataset, none of these studies has reported an increase in diatom biomass; instead, modest increases were attributed to non-diatom eukaryotes (AEUKs). *Haulani* showed a three-fold increase in fucoxanthin standing stock, but the increase was due to growth of prymnesiophytes, and the average biovolume of diatoms was actually smaller in the eddy relative to ambient species (Vaillancourt et al., 2003).

One explanation for these differences in phytoplankton communities is that we may have sampled Cyclone *Opal* at an eddy life cycle stage not previously encountered. Alternatively, other studies may simply have missed blooms, given the relatively narrow core regions of eddies and the rapid decline of diatom populations. If diatom blooms were a ubiquitous feature of Hawaiian lee cyclones, however, it seems unlikely that previous studies would have found enhanced populations of other taxa, without any evidence of diatoms or senescent layers indicative of past blooms. Because eddies of similar age can have very different biological characteristics (Rii et al., 2008), we need to re-examine the concept of an eddy life cycle (Sweeney et al., 2003) as it applies to the structure and dynamics of plankton communities.

Given proximity to the islands, it is not unreasonable to suspect that the unique diatom bloom in Cyclone *Opal* may have been due to a seed population from coastal waters. However, there was no unusual salinity signature in *Opal*'s center, and no other biological indications of entrained coastal waters. Salinity profiles show classic uplifted isohalines and surface outcropping (Dickey et al., 2008).

Even when macronutrient concentrations are comparable between eddies, their rates of input can vary considerably. Differences in spin-up times can lead to different input rates, while open and closed eddy systems differ with regard to single perturbations versus continuous fluxes. Rapid or pulsed nutrient fluxes select for centric diatom populations (high V_{max}), whereas a more continuous nutrient supply selects for flagellates (low K_s) (Parsons and Takahashi, 1973; Turpin and Harrison, 1979). As a result, rapidly generated eddies with a high nutrient flux should select for diatoms, and slower developing eddies with a lower rate of nutrient input should select for flagellated forms. Unfortunately, the subsurface genesis of cyclonic eddies makes it difficult to estimate the spin-up times necessary to explore this hypothesis.

Closed eddies assume a single pulse of nutrient input from the doming isopycnals with no subsequent horizontal exchange. Open eddies, on the other hand, allow horizontal exchange along density surfaces and continuous supply of nutrients. Based on phytoplankton uptake kinetics, we expect a diatom-dominated community to develop in a closed system with a large nutrient pulse, and a flagellate dominated community in an open system with a continuous low nutrient supply. In fact, the structure of the phytoplankton community in Cyclone *Opal* is consistent with both the open-bottom, closed-core hypothesis (Nencioli et al., 2008) and the expected relationship between nutrient flux and community structure (Turpin and Harrison, 1979). Thus, diatoms dominated the isolated central core of the eddy, which received a pulse of nutrients, whereas flagellates (AEUKs) dominated the chl max outside of the eddy subject to isopycnal mixing and continuous nutrient inputs.

4.3. Diatoms in the desert?

Ours is not the first observation of enhanced diatom abundance in the North Pacific subtropical gyre (NPSG). For example, notable concentrations have been reported from early studies at the CLIMAX station (Venrick, 1974), from time-series sampling at Stn ALOHA (Scharek et al., 1999a, b), from a cyclonic eddy in the vicinity of Stn ALOHA (Brzezinski et al., 1998), and as a frequent occurrence in the area of 28–30°N 130–160°W based on satellite data (Wilson, 2003). None of these studies, however, has shown diatoms to account for more than 20% of phytoplankton biomass (Scharek et al., 1999b). Furthermore, Venrick (1974) has noted that "these localized areas of increased phytoplankton biomass may be as close to a bloom as this impoverished environment is capable of supporting".

Previous observations of weak diatom blooms in the NPSG have attributed them to three genera: *Rhizosolenia* spp., *Hemiaulus* spp. and *Mastogloia* spp. (Venrick, 1969, 1974). All of these genera are lightly silicified with a high affinity for silicic acid or low cell quota (Brzezinski et al., 1998), and are associated with the nitrogen-fixing endosymbiont *Richelia*. Diatoms in the NPSG are thus more associated with their unique strategy for living under oligotrophic conditions, than their dynamic responses to nutrient perturbations. In contrast, diatoms comprising the subsurface bloom in Cyclone *Opal* were large and robust forms without symbionts. They achieved biomass levels nearly two orders of magnitude over background and strongly dominated (85%) phytoplankton biomass. In cell types, diversity, biomass, magnitude and % community dominance, *Opal* bloom diatoms more closely resembled the results of the SOFeX iron fertilization bloom in the Southern Ocean (Coale et al., 2004), than anything previously seen in the NPSG.

Approximately, 22 genera of diatoms occur in the NPSG (Venrick, 1969, 1979; Scharek et al., 1999a, b). All could be found in a single sample of a few hundred milliliters in the center of Cyclone *Opal*. While approximately 50% of the diatom biomass was attributed to *Chaetoceros* and *Rhizosolenia* spp., the remaining fraction comprised a surprising array of species, a small sample of which is depicted in Fig. 9. *Corethron* spp., for example, were abundant in the eddy. These are large conspicuous species and easy to identify; to our knowledge, they have not previously been reported in these waters.

We are also only the second report of colonial *Phaeocystis* spp. in the NPSG, the other from Station ALOHA in 1994 (Venrick, 1997). Often considered a nuisance flagellate, *Phaeocystis* spp. frequently occurs after nutrient inputs or shifts in nutrient ratios (Smayda, 1990; Hegarty and Villareal, 1998); its presence in a nutrient-enriched eddy is therefore not surprising. *Phaeocystis* spp. is notable as a potential contributor to export, with a mucus-rich colonial form that facilitates aggregation and sinking (Wassmann, 1994). Small *Phaeocystis* colonies have also been reported to attach to *Chaetoceros* cells (Rousseau et al., 1994), which is consistent with its presence in the *Chaetoceros*-rich chl max of *Opal*. However, *Phaeocystis* was not limited to the surface of diatom cells as colonies were also found in the surface mixed layer of the eddy. The presence of *Phaeocystis* spp. is often linked in succession with diatoms in response to nutrient limitation (Veldhuis et al., 1986), presumably from Si depletion in Cyclone *Opal* (Benitez-Nelson et al., 2007; Rii et al., 2008).

4.4. Overprinting versus succession

Barber and Hiscock (2006) recently challenged the notion of dramatic successional changes in community composition during open-ocean diatom blooms. The basis of their argument, drawn primarily from the results of iron fertilization experiments, is that non-diatom populations, specifically small pico- and nanoplankton, often change little in response to nutrient addition. However, they are overwhelmed by the diatom response such that their declining relative contributions to community biomass give the appearance of replacement by succession. According to Barber and Hiscock (2006), a general increase in standing stocks of ambient phytoplankton would be predicted in the center of Cyclone *Opal* due to favorable growth conditions, and diatom biomass added to the existing community. Thus, the ambient community would be "overprinted", rather than replaced by the diatom bloom (Landry et al., 1997).

While modest in comparison to the accumulation of diatoms, the biomass of other photosynthetic eukaryotes (AEUK) was about 50% higher in Cyclone *Opal* than OUT stations (Fig. 2 and Table 1), as were smaller ($<5\,\mu m$) cells more typical of ambient populations (data not shown). Depth-integrated concentrations of 19′-hexanoyloxyfucoxanthin and 19′-butanoyloxyfucoxanthin (pigment indicators of prymnesiophytes and pelagophytes, respectively) were similar in the center of *Opal* and OUT stations (Rii et al., 2008). Furthermore, AEUK biomass declined with diatom abundance (Fig. 6), rather than showing an inverse response indicative of succession. Thus, for eukaryotic populations, the Barber and Hiscock (2006) argument appears to hold true.

For prokaryotic picophytoplankton, PRO and SYN abundances were relatively constant in the upper mixed layer (40 m) of *Opal* and similar to OUT sites (Table 1), and growth rates of PRO were significantly enhanced and balanced by increased grazing in this stratum at the eddy center (Landry et al., 2008). Consistent with prediction, therefore, the observed increases in diatoms in the central mixed layer of Cyclone *Opal* were overprinted on the increased biomass of the ambient community of picophytoplankton. However, PRO abundance and growth rate were both significantly depressed relative to OUT stations in the subsurface diatom bloom of the eddy (Table 1). Reduced deep-water populations of PRO also were reflected in depth-integrated concentrations of divinyl chlorophyll *a* and zeaxanthin (pigment indicators of PRO and cyanobacteria, respectively), which were substantially lower in the center of the eddy (Rii et al., 2008). At depth, the marked decrease in growth rates and standing stocks of ambient picophytoplankton, concurrent with the dramatic increase in diatom biomass suggests complex plankton community interactions, if not succession, beyond simple overprinting.

In Barber and Hiscock's (2006) analysis, the limiting resource for diatom growth was iron, an essential micronutrient that benefits all phytoplankton. The iron was added to the upper mixed layer, so the perturbations involved assemblages adapted to a high

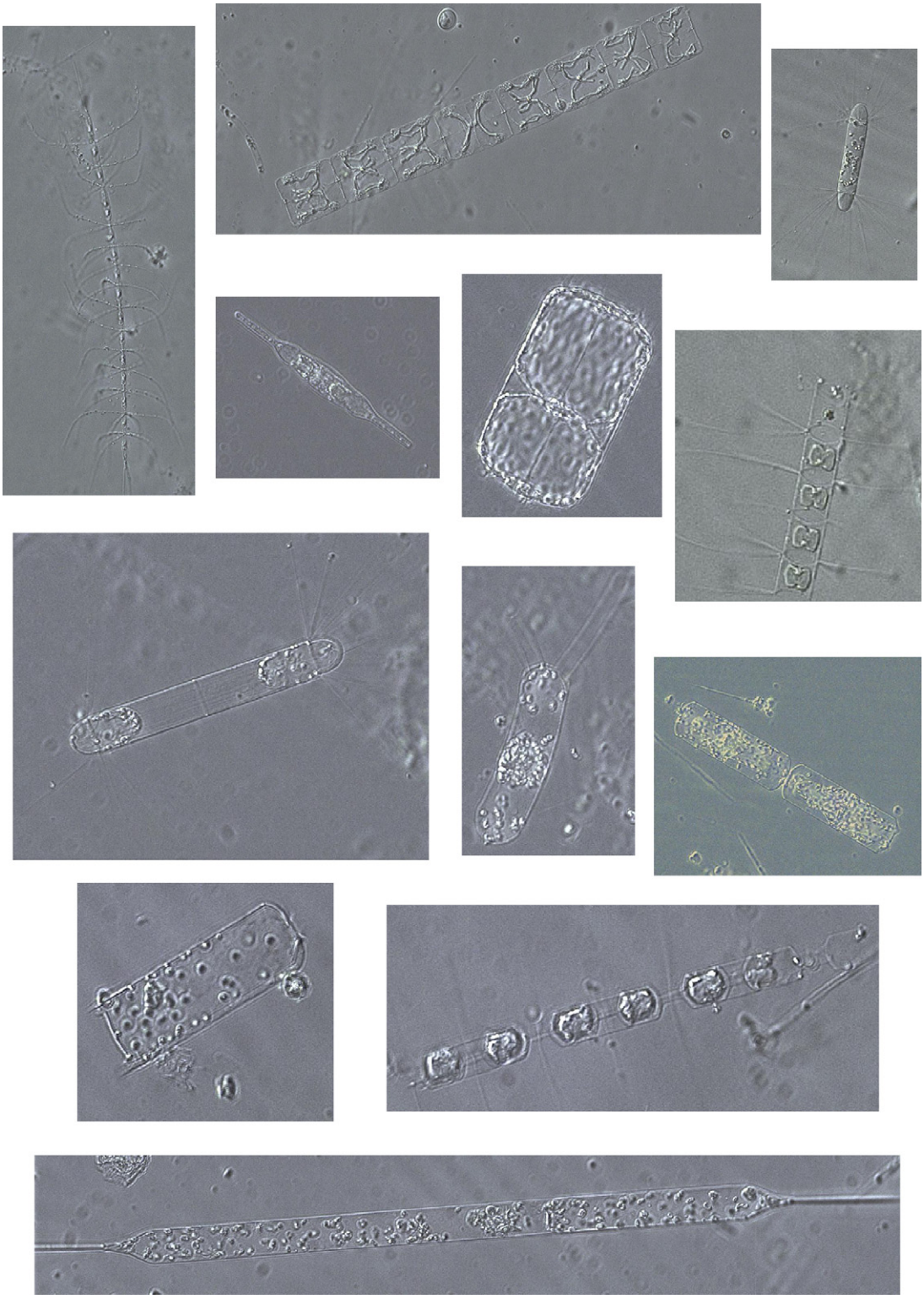

Fig. 9. Photomicrographs illustrating the diversity of diatoms found in the center of the eddy. All photos taken from the same sample; magnification varies and sizes are not to scale. Cells were preserved in 0.5% paraformaldehyde.

light environment. In Cyclone *Opal*, however, upwelled macronutrients were the primary limiting resource for diatom growth, with light playing a secondary role as accumulating bloom concentrations in the uplifted nutricline (40–60 m) reduced the depth of light penetration below. Since PRO lacks the ability to utilize nitrate (Moore et al., 2002), it would not be able to benefit immediately, and may even have been negatively impacted as low-light adapted PRO were uplifted from the ambient deep euphotic zone to high light. As grazing increased in the bloom stratum, the enhanced flux of recycled ammonium might have improved the resource environment for PRO, but the light regime in the bloom by then would have resembled that at much deeper

depths in ambient waters, selecting for low-light PRO with slower growth rates. Viewed in this manner, the lower growth rate and reduced abundance of PRO in the eddy bloom do not necessarily suggest a succession of PRO to diatoms, but rather a contraction of the euphotic zone, with slower growing, low-light adapted PRO species occurring much shallower in the water column than at ambient OUT stations (e.g., Fig. 3). With consideration for the complexities of the growth environment and the relevant populations, therefore, we can reasonably reconcile the seemingly disparate observations of PRO and diatoms in the eddy bloom to the overprinting prediction of Barber and Hiscock (2006). In this case, diatoms overprinted low-light PRO from the deep euphotic zone, rather than the high-light form that dominates at the depth of the diatom bloom (50–80 m) in the ambient environment.

5. Conclusions

Cyclone *Opal* was a well-developed and physically stable eddy with a dynamic and evolving biology. We found a dramatic subsurface bloom of large diatoms, unprecedented for this oligotrophic region, in the 40 km central core region of shoaling isopycnal surfaces. In addition to enriching the bloom stratum, the eddy also stimulated higher levels of phytoplankton and heterotrophic biomass in the overlying mixed layer. In most respects, *Opal's* bloom response appeared to be superimposed upon rather than replacing the ambient community, though it modified the depth distributions of ambient populations by reducing light penetration. As the bloom declined, however, the diatom assemblage underwent a successional transition to species more characteristic of oligotrophic waters. Differences between the plankton response in Cyclone *Opal* and Hawaiian lee eddies from previous studies point to the rate of formation, subsequent rate of nutrient flux, and/or the degree of mixing with surrounding waters as possible factors shaping phytoplankton community structure within eddies. The diatom bloom of Cyclone *Opal* was a unique, and possibly extreme, example of biological response to physical forcing in the North Pacific subtropical gyre, and its detailed study may therefore help to improve our predictive understanding of environmental controls on plankton community structure.

Acknowledgments

We thank the captain and crew of the R/V *Wecoma* for logistical support, and all E-Flux participants for their input and contributions, particularly Melinda Simmons for her assistance at sea. This work was funded by NSF Grants 0241897 and 0324666 and is contribution number 7454 from the School of Ocean and Earth Science and Technology at the University of Hawaii at Manoa.

References

Allen, C.B., Kanda, J., Laws, E.A., 1996. New production and photosynthetic rates within and outside a cyclonic mesoscale eddy in the North Pacific Subtropical Gyre. Deep-Sea Research I 43, 917–936.

Barber, R.T., Hiscock, M.R., 2006. A rising tide lifts all phytoplankton: growth response of other phytoplankton taxa in diatom-dominated blooms. Global Biogeochemical Cycles 20, GB4S03.

Benitez-Nelson, C.R., Bidigare, R.R., Dickey, T., Landry, M.R., Leonard, C.L., Brown, S.L., Nencioli, F., Rii, Y.M., Maiti, K., Becker, J.W., Bibby, T.S., Black, W., Cai, W.-J., Carlson, C., Chen, F., Kuwahara, V.S., Mahaffey, C., McAndrew, P.M., Quay, P.D., Rappe, M.S., Selph, K.E., Simmons, M.E., Yang, E.J., 2007. Eddy-induced diatom bloom drives increased biogenic silica flux, but inefficient carbon export in the subtropical North Pacific Ocean. Science 316, 1017–1021.

Bibby, T.S., Gorbunov, M.Y., Wyman, K.W., Falkowski, P.G., 2008. Photosynthetic community responses to upwelling mesoscale eddies in the subtropical north Atlantic and Pacific Oceans. Deep-Sea Research II, this issue [doi:10.1016/j.dsr2.2008.01.014].

Bidigare, R.R., Trees, C.C., 2000. HPLC phytoplankton pigments: sampling, laboratory methods, and quality assurance procedures. In: Mueller, J.L., Gargion, G. (Eds.), Ocean Optics Protocols for Satellite Ocean Color Sensor Validation, Revision 2, NASA Technical Memo, 2000209966, pp. 154–161.

Bidigare, R.R., Benitez-Nelson, C., Leonard, C.L., Quay, P.D., Parsons, M.L., Foley, D.G., Seki, M.P., 2003. Influence of a cyclonic eddy on microheterotroph biomass and carbon export in the lee of Hawaii. Geophysical Research Letters 30, 51–54.

Bidigare, R.R., Van Heukelem, L., Trees, C.C., 2005. Analysis of algal pigments by high-performance liquid chromatography. In: Andersen, R. (Ed.), Algal Culturing Techniques. Academic Press, pp. 327–345.

Binder, B.J., DuRand, M.D., 2002a. Diel cycles in surface waters of the equatorial Pacific. Deep-Sea Research II 49, 2601–2617.

Binder, B.J., DuRand, M.D., 2002b. Diel cycles in surface waters of the equatorial Pacific. Deep-Sea Research II 49, 2601–2618.

Boyd, P., Doney, S., 2002. Modeling regional responses by marine pelagic ecosystems to global climate change. Geophysical Research Letters 29.

Boyd, P.W., Law, C.S., 2001. The Southern Ocean Iron RElease Experiment (SOIREE); introduction and summary. Deep-Sea Research II 48 (11–12), 2425–2438.

Brzezinski, M., Villareal, T., Lipschultz, F., 1998. Silica production and the contribution of diatoms to new and primary production in the central North Pacific. Marine Ecology Progress Series 167, 89–104.

Campbell, L., Vaulot, D., 1993. Photosynthetic picoplankton community structure in the subtropical North Pacific Ocean near Hawaii (station ALOHA). Deep-Sea Research I 40, 2043–2060.

Campbell, L., Nolla, H.A., Vaulot, D., 1994. The importance of *Prochlorococcus* to community structure in the central North Pacific Ocean. Limnology and Oceanography 39, 954–961.

Chavanne, C., Flament, P., Lumpkin, R., Dousset, B., Bentamy, A., 2002. Scatterometer observations of wind variations by oceanic islands: implications for wind driven ocean circulation. Canadian Journal on Remote Sensing 28 (3), 466–474.

Cipollini, P., Cromwell, D., Challenor, P.G., Raffaglio, S., 2001. Rossby waves detected in global ocean colour data. Geophysical Research Letters 28, 466–474.

Coale, K.H., Johnson, K.S., Fitzwater, S.E., Gordon, R.M., Tanner, S., Chavez, F.P., Ferioli, L., Sakamoto, C., Rogers, P., Millero, F., Steinberg, P., Nightingale, P., Cooper, D., Cochlan, W.P., Landry, M.R., Constantinou, J., Rollwagen, G., Trasvina, A., Kudela, R., 1996. A massive phytoplankton bloom induced by an ecosystem-scale iron fertilization experiment in the equatorial Pacific Ocean. Nature 383, 495–501.

Coale, K.H., Johnson, K.S., Chavez, F.P., Buesseler, K.O., Barber, R.T., Brzezinski, M.A., Cochlan, W.P., Millero, F.J., Falkowski, P.G., Bauer, J.E., Wanninkhof, R.H., Kudela, R.M., Altabet, M.A., Hales, B.E., Takahashi, T., Landry, M.R., Bidigare, R.R., Wang, X., Chase, Z., Strutton, P.G., Friederich, G.E., Gorbunov, M.Y., Lance, V.P., Hilting, K.P., Hiscock, M.R., Demarest, M., Hiscock, W.T., Sullivan, K.F., Tanner, S.J., Gordon, R.M., Hunter, C.N., Elrod, V.A., Fitzwater, S.E., Jones, J.L., Tozzi, S., Koblizek, M., Roberts, A.E., Herndon, J., Brewster, J., Ladizinsky, N., Smith, G., Cooper, D., Timothy, D., Brown, S.L., Selph, K.E., Sheridan, C.C., Twining, B.S., Johnson, Z.I., 2004. Southern Ocean iron enrichment experiment; carbon cycling in high- and low-Si waters. Science 304, 408–414.

Dickey, T., Nencioli, F., Kuwahara, V., Leonard, C., Black, W., Bidigare, R., Rii, Y., Zhang, Q., 2008. Physical and bio-optical observations of oceanic cyclones west of the island of Hawai'i. Deep-Sea Research II, this issue [doi:10.1016/j.dsr2.2008.01.006].

DuRand, M.D., Olson, R.J., 1996. Contributions of phytoplankton light scattering and cell concentration changes to diel variations in beam attenuation in the equatorial Pacific from flow cytometric measurements of pico-, ultra-, and nanoplankton. Deep-Sea Research II 43, 891–906.

DuRand, M.D., Olson, R.J., 1998. Diel patterns in optical properties of the chlorophyte *Nannochloris* sp.: relating individual-cell to bulk measurements. Limnology and Oceanography 43, 1107–1118.

Edler, L., 1979. Phytoplankton and chlorophyll recommendations for biological studies in the Baltic Sea. In: Recommendations on methods for marine biological studies in the Baltic Sea: phytoplankton and chlorophyll. Baltic Marine Biologists 5, 13–25.

Eppley, R.W., Reid, F.M.H., Strickland, J.D.H., 1970. Estimates of phytoplankton crop size, growth rate, and primary production. In: Strickland, H.J.D. (Ed.), The Ecology of the Plankton off La Jolla California in the Period April Through September, 1967. Bulletin of Scripps Institution of Oceanography 17, 33–42.

Falkowski, P.G., Ziemann, D., Kolber, Z., Bienfang, P.K., 1991. Role of eddy pumping in enhancing primary production in the ocean. Nature 352, 55–58.

Garrison, D.L., Gowing, M.M., Hughes, M.P., Campbell, L., Caron, D.A., Dennett, M.R., Shalapyonok, A., Olson, R.J., Landry, M.R., Brown, S.L., Liu, H., Azam, F., Steward, G.F., Ducklow, H.W., Smith, D.C., 2000. Microbial food web structure in the Arabian Sea: a US JGOFS study. Deep-Sea Research II 47, 1387–1422.

Harrison, P.J., 2006. SERIES (subarctic ecosystem response to iron enrichment study): a Canadian-Japanese contribution to our understanding of the iron-ocean-climate connection. Deep-Sea Research II 53, 2006–2011.

Hegarty, S.G., Villareal, T.A., 1998. Effects of light level and N:P supply ratio on the competition between *Phaeocystis cf. pouchetii* (Hariot) Legerheim (Prymnesiophyceae) and five diatom species. Journal of Experimental Marine Biology and Ecology 226, 241–258.

Karl, D.M., Bidigare, R.R., Letelier, R.M., 2001. Long term changes in plankton community structure and productivity in the North Pacific Subtropical Gyre: the domain shift hypothesis. Deep-Sea Research II 48, 1449–1470.

Landry, M.R., Barner, R.T., Bidigare, R.R., Chai, F., Coale, K., Dam, H., Lewis, M., Lindley, S.T., McCarthy, J.J., Roman, M.R., Stoecker, D.K., Verity, P.G., White, J.R., 1997. Iron and grazing constraints on primary production in the central equatorial Pacific: an EqPac synthesis. Limnology and Oceanography 42 (3), 405–418.

Landry, M.R., Brown, S.L., Rii, Y.M., Selph, K.E., Bidigare, R.R., Yang, E.J., Simmons, M.P., 2008. Depth-stratified phytoplankton dynamics in Cyclone *Opal*, a subtropical mesoscale eddy, this issue [doi:10.1016/j.dsr2.2008.02.001].

Le Quéré, C., Harrison, S.P., Prentice, I.C., Buitenhuis, E.T., Aumont, O., Bopp, L., Claustre, H., Da Cunha, L.C., Geider, R., Giraud, X., Klaas, C., Kohfeld, K.E., Legendre, L., Manizza, M., Platt, T., Rivkin, R.B., Sathyendranath, S., Uitz Watson, A.J., Wolf-Gladrow, D., 2005. Ecosystem dynamics based on plankton functional types for global ocean biogeochemistry models. Global Change Biology 11, 1–25.

Legendre, L., Le Fevre, J., 1995. Microbial food webs and the export of biogenic carbon in oceans. Aquatic Microbial Ecology 9, 69–77.

Legendre, L., Michaud, J., 1998. Flux of biogenic carbon in oceans: size-dependent regulation by pelagic food webs. Marine Ecology Progress Series 164, 1–11.

Legendre, L., Rivkin, R., 2000. Cycling of biogenic carbon in oceans: regulation by food-web control nodes. In: Joint Global Ocean Flux Study—Open Science Conference—Ocean Biogeochemistry: A New Paradigm. Bergen, Norway, pp. 13–17, 85–86.

Lobel, P.S., Robinson, A.R., 1986. Transport and entrapment of fish larvae by ocean mesoscale eddies and currents in Hawaiian waters. Deep-Sea Research 33 (4), 483–500.

Lumpkin, C.F., 1998. Eddies and currents in the Hawaiian Islands. Ph.D. Thesis, University of Hawaii, 281pp.

Mantoura, R.F.C., Llewellyn, C.A., 1983. The rapid determination of algal chlorophyll and carotenoid pigments and their breakdown products in natural waters by reverse-phase high-performance liquid chromatography. Analytica Chimica Acta 151, 297–314.

Menden-Deuer, S., Lessard, E.J., 2000. Carbon to volume relationships for dinoflagellates, diatoms and other protist plankton. Limnology and Oceanography 45, 569–579.

Michaels, F., Silver, M.W., 1988. Primary production, sinking fluxes and the microbial food web. Deep-Sea Research 35, 473–490.

Michaels, A.F., Caron, D.A., Swanberg, N.R., Howse, F.A., Michaels, C.M., 1995. Planktonic sarcodines (Acantharia, Radiolaria, Foraminifera) in surface waters near Bermuda: abundance, biomass and vertical flux. Journal of Plankton Research 17, 131–163.

Monger, B.C., Landry, M.R., 1993. Flow cytometric analysis of marine bacteria with Hoechst 33342. Applied Environmental Microbiology 59, 905–911.

Moore, L.R., Post, A.F., Rocap, G., Chisholm, S.W., 2002. Utilization of different nitrogen sources by the marine cyanobacteria *Prochlorococcus* and *Synechococcus*. Limnology and Oceanography 47, 89–996.

Nencioli, F., Kuwhara, V.S., Dickey, T.D., Rii, Y.M., Bidigare, R.R., 2008. Physical dynamics and biological implications of a mesoscale eddy in the lee of Hawai'I: Cyclone *Opal* observations during E-Flux III. Deep-Sea Research II, this issue [doi:10.1016/j.dsr2.2008.02.003].

Olaizola, M., Ziemann, D.A., Bienfang, P.K., Walsh, W.A., Conquest, L.D., 1993. Eddy-induced oscillations of the pycnocline affect the floristic composition and depth distribution of phytoplankton in the subtropical Pacific. Marine Biology 116, 533–542.

Parsons, T.R., Takahashi, M., 1973. Environmental control of phytoplankton cell size. Limnology and Oceanography 18, 511–515.

Patzert, W.C., 1969. Eddies in Hawaiian waters. HIG Technical Report 69-8, Hawaii Institute of Geophysics, University of Hawaii.

Putt, M., Stoecker, D.K., 1989. An experimentally determined carbon: volume ratio for marine "oligotrichous" ciliates from estuarine and coastal waters. Limnology and Oceanography 34, 1097–1103.

Rii, Y.M., Brown, S.L., Nenciolo, F., Kuwahara, V., Dickey, T.D., Karl, D.M., Bidigare, R.R., 2008. The transient oasis: Nutrient-phytoplankton dynamics and particle export in Hawaiian lee cyclones. Deep-Sea Research II, this issue [doi:10.1016/j.dsr2.2008.01.013].

Rousseau, V., Vaulot, D., Casotti, R., Cariou, V., Lenz, J., Gunkel, J., Baumann, M.E.M., 1994. The life cycle of *Phaeocystis pouchetii* in the Eastern Irish Sea. Journal of Marine Biology Association of the United Kingdom 70, 249–253.

Sakamoto, C.M., Karl, D.M., Jannasch, H.W., Bidigare, R.R., Letelier, R.M., Walz, P.M., Ryan, J.P., Polito, P.S., Johnson, K.S., 2004. Influence of Rossby waves on nutrient dynamics and the plankton community structure in the North Pacific subtropical gyre. Journal of Geophysical Research 109.

Scharek, R., Latasa, M., Karl, D.M., Bidigare, R.R., 1999a. Temporal variations in diatom abundance and downward flux in the oligotrophic North Pacific gyre. Deep-Sea Research I 46, 1051–1075.

Scharek, R., Tupas, L.M., Karl, D.M., 1999b. Diatom fluxes to the deep-sea in the oligotrophic North Pacific gyre at Station ALOHA. Marine Ecology Progress Series 182, 55–67.

Schlitzer, R., 2006. Ocean Data View, 〈http://odv.awi.de〉.

Seki, M.P., Polovina, J.J., Brainard, R.E., Bidigare, R.R., Leonard, C.L., Foley, D.G., 2001. Biological enhancement at cyclonic eddies tracked with GOES thermal imagery in Hawaiian waters. Geophysical Research Letters 28, 1583–1586.

Seki, M.P., Lumpkin, R., Flament, P., 2002. Hawaii cyclonic eddies and blue marlin catches: the case study of the 1995 Hawaiian International Billfish Tournament. Journal of Oceanography 58 (5), 739–745.

Sherr, E.B., Sherr, B.F., 1993. Preservation and storage of samples for enumeration of heterotrophic protests. In: Kemp, P.K., et al. (Eds.), Handbook of Methods in Aquatic Microbial Ecology. CRC Press, Boca Raton, FL, pp. 207–212.

Smayda, T., 1990. Novel and nuisance phytoplankton blooms in the sea: evidence for a global epidemic. In: Granéli, E., Sundström, B., Edler, L., Anderson, D.M. (Eds.), Toxic Marine Phytoplankton. Elsevier, New York, pp. 21–41.

Strathmann, R.R., 1967. Estimating the organic carbon content of phytoplankton from cell volume or plasma volume. Limnology and Oceanography 36, 50–63.

Sweeney, E.N., McGillicuddy, D.J., Buesseler, K.O., 2003. Biogeochemical impacts due to mesoscale eddy activity in the Sargasso Sea as measured at the Bermuda Atlantic Time-series Study (BATS). Deep-Sea Research Part II 50, 3017–3039.

Tsuda, S.T., Saito, H., Nishioka, J., Nojiri, Y., Kudo, I., 2003. A mesoscale iron enrichment in the western subarctic Pacific induces a large centric diatom bloom. Science 300, 958–961.

Turpin, D.H., Harrison, P.J., 1979. Limiting nutrient patchiness and its role in phytoplankton ecology. Journal of Experimental Marine Biology and Ecology 39, 151–166.

Uz, B.M., Yoder, J.A., Osychny, V., 2001. Pumping of nutrients to ocean surface waters by the action of propogating waves. Nature 409, 597–600.

Vaillancourt, R., Marra, J., Seki, M., Parsons, M., Bidigare, R.R., 2003. Impact of a cyclonic eddy on phytoplankton community structure and photosynthetic competency in the subtropical North Pacific Ocean. Deep-Sea Research I 50, 829–847.

Veldhuis, M.J.W., Coljin, F., Admiraal, W., 1986. The spring bloom of Phaeocystis pouchetii (Haptophyceae). Netherlands Journal of Sea Research 20, 37–48.

Venrick, E.L., 1969. The distribution and ecology of oceanic diatoms in the North Pacific. PhD Thesis, University of California San Diego, 694pp.

Venrick, E.L., 1974. The distribution and significance of *Richelia intracellularis* Schmidt in the North Pacific central gyre. Limnology and Oceanography 19, 437–445.

Venrick, E.L., 1979. The lateral extent and characteristics of the North Pacific central environment at 35″N. Deep-Sea Research 26, 1153–1178.

Venrick, E.L., 1997. Comparison of the phytoplankton species structure in the Climax area (1973–1985) with that of station ALOHA. Limnology and Oceanography 42 (7), 1643–1648.

Venrick, E.L., 1999. Phytoplankton species structure in the central North Pacific, 1973–1996: variability and persistence. Journal of Plankton Research 21 (6), 1029–1042.

Verity, P.G., Langdon, C., 1984. Relationship between lorica volume, carbon, nitrogen, and ATP content of tintinnids in Narragansett Bay. Journal of Plankton Research 66, 859–868.

Wassmann, P., 1994. Significance of sedimentation for the termination of Phaeocystis blooms. Journal of Marine Systems 5, 81–100.

Wilson, C., 2003. Late Summer chlorophyll blooms in the oligotrophic North Pacific Subtropical Gyre. Geophysical Research Letters 30, 1942.

Wright, S.W., Jeffrey, S.W., Mantoura, R.F.C., Llewellyn, C.A., Bjornland, T., Repeta, D., Welschmeyer, N., 1991. Improved HPLC method for the analysis of chlorophylls and carotenoids from marine phytoplankton. Marine Ecology Progress Series 77, 183–196.